

5-16-2007

Sequence specific electronic conduction through polyion-stabilized double-stranded DNA in nanoscale break junctions

Ajit K. Mahapatro

Birck Nanotechnology Center, School of Electrical and Computer Engineering, Purdue University, ajit@purdue.edu

Kyung J. Jeong

Birck Nanotechnology Center, Departments of Chemical and Biomedical Engineering, Purdue University, jeongk@purdue.edu

Gil U. Lee

Birck Nanotechnology Center, Departments of Chemical and Biomedical Engineering, Purdue University, gl@atom.ecn.purdue.edu

David B. Janes

Birck Nanotechnology Center, School of Electrical and Computer Engineering, Purdue University, david.b.janes.1@purdue.edu

Follow this and additional works at: <http://docs.lib.purdue.edu/nanodocs>

Mahapatro, Ajit K.; Jeong, Kyung J.; Lee, Gil U.; and Janes, David B., "Sequence specific electronic conduction through polyion-stabilized double-stranded DNA in nanoscale break junctions" (2007). *Other Nanotechnology Publications*. Paper 21.
<http://docs.lib.purdue.edu/nanodocs/21>

This document has been made available through Purdue e-Pubs, a service of the Purdue University Libraries. Please contact epubs@purdue.edu for additional information.

Sequence specific electronic conduction through polyion-stabilized double-stranded DNA in nanoscale break junctions

Ajit K Mahapatro¹, Kyung J Jeong², Gil U Lee² and David B Janes^{1,3}

¹ Birk Nanotechnology Center, School of Electrical and Computer Engineering, Purdue University, West Lafayette, IN 47907, USA

² Birk Nanotechnology Center, Departments of Chemical and Biomedical Engineering, Purdue University, West Lafayette, IN 47907, USA

E-mail: ajit@ecn.purdue.edu, gl@purdue.edu and janes@ecn.purdue.edu

Received 29 December 2006, in final form 1 February 2007

Published 17 April 2007

Online at stacks.iop.org/Nano/18/195202

Abstract

This paper presents a study of sequence specific electronic conduction through short (15-base-pair) double-stranded (ds) DNA molecules, measured by immobilizing 3'-thiol-derivatized DNAs in nanometre scale gaps between gold electrodes. The polycation spermidine was used to stabilize the ds-DNA structure, allowing electrical measurements to be performed in a dry state. For specific sequences, the conductivity was observed to scale with the surface density of immobilized DNA, which can be controlled by the buffer concentration. A series of 15-base DNA oligonucleotide pairs, in which the centre sequence of five base pairs was changed from G:C to A:T pairs, has been studied. The conductivity per molecule is observed to decrease exponentially with the number of adjacent A:T pairs replacing G:C pairs, consistent with a barrier at the A:T sites. Conductance-based devices for short DNA sequences could provide sensing approaches with direct electrical readout, as well as label-free detection.

1. Introduction

The electronic properties of polynucleotides have drawn significant interest over the past two decades due to the central role they play in biology and the precise manner in which they can be used to control structure at the nanometre scale. The electron transfer properties of single- and double-stranded DNA oligonucleotides have been used to enable electrochemical detection of arrays of DNA sequences [1–4]. The development of devices suitable for measuring the electrical conductivity of short DNA sequences could provide sensing approaches with direct electrical readout, which would facilitate integration of the sensor with control and signal processing circuitry, as well

as label-free detection. If these devices can operate at a few-molecule level, they could eliminate the need for amplification techniques such as polymerase chain reaction (PCR). The ability to synthesize specific DNA sequences has also made it possible to form novel nanostructures from DNA oligonucleotides and composites [5–8]. These structures may have biotechnological applications but also have several promising materials applications.

Electron transfer and electrical transport experiments have been carried out to understand the mechanism of the electrical conduction through ds-DNAs. Electron transfer experiments [9–11] involve the transfer of charge from one end of the molecule to the other, but no net flow of charge or associated current between contacts and the molecule. Experimental techniques include

³ Author to whom any correspondence should be addressed.

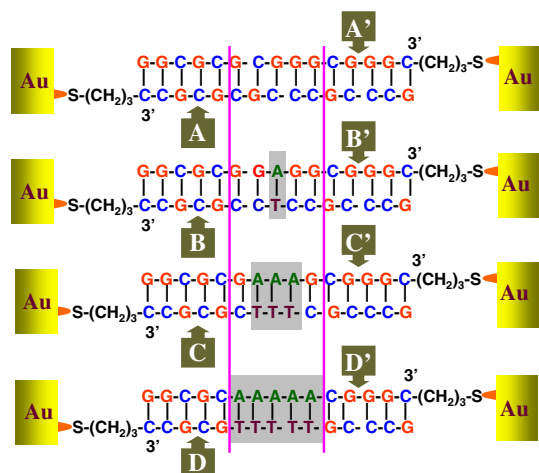


Figure 1. Structures of the four dithiol-derivatized ds-DNAs used in this study.

chemical doping [11, 12] using oxidation–reduction processes, photoinduced charge transfer [9, 13], and microwave-radiation-induced excitations [14]. The charge migration mechanisms which have been inferred from the electron transfer rate experiments [15] are ‘coherent tunnelling’ [10] in ds-DNAs over a length of a few base pairs, and ‘diffusive thermal hopping’ in ds-DNAs longer than a few nanometres. In longer DNA, i.e. longer than $1\ \mu\text{m}$ in length, defects induced by the surface force field reduce the efficient charge migration through the DNA backbone.

Electron transport experiments [16, 17] typically involve electrical contacts, usually metal, at the two ends of the molecule, and the observation of net current flow through the molecule in response to an applied voltage between the contacts. Transport experiments and theoretical studies on longer ds-DNAs show electrically insulating behaviour [17–19]. However, DNA bundles [20], networks [21], and short ds-DNAs, i.e. shorter than 40 nm in length [16, 17], show significant conduction. Various approaches have been developed to measure the conductance through short ds-DNAs in aqueous solution as well as in their dry state using techniques with various contact structures, including aligned film casting [25], electrical break junction [26], and scanning probe microscopy [16]. Electronic transport studies have generally not addressed the issue of sequence specific conductance, which would be crucial for any conductance based sensor applications. This lack of attention to the specific structure is one of the factors that contribute to the apparent inconsistencies between various reports of conductance levels.

The influence of molecule–electrode binding on single molecule conductance is also significant [22] because the surface binding energy can be strong enough to distort the electronic structure [23], especially in a complex system like DNA where the electronic structure [24] and electrical conductivity are sequence and length dependent. To understand the conductance and transport mechanisms through DNA, appropriate metal–DNA contacts must be realized at both ends of the DNA. Ideally, contacts would have a negligible effect on electrical measurements compared to the interstrand interactions, i.e. hydrogen-bonded purine–pyridine

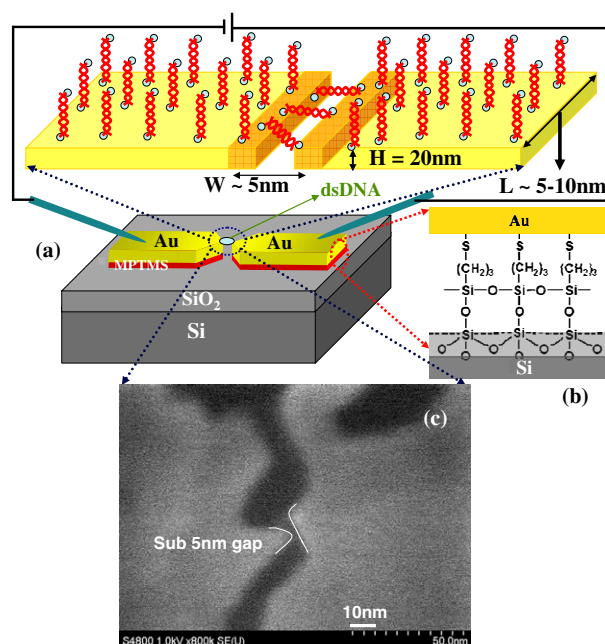


Figure 2. Schematic diagrams of (a) the test device to measure ds-DNA conduction, (b) Au micro-wires formed using MPTMS molecular adhesion layer on SiO_2 . (c) FESEM image of a molecular scale gap between a pair of Au electrodes formed through electromigration at room temperature. The highlighted area represents the active area of the junction, i.e. the area where the gap length is comparable to the length of the ds-DNA.

base pairings and base stacking, and intrastrand interactions, i.e. covalently bonded phosphate groups with the 3' and 5' hydroxyl groups of deoxyribose sugars in the DNA backbone.

This paper describes a study of electrical conduction through 15-base-pair oligonucleotides in which the sequence of the strands has been systematically varied. These measurements have been enabled through the recent development of a technique [27] to reproducibly form pairs of gold (Au) electrodes that are separated by a gap length comparable to the length of the ds-DNA molecules. Metal/DNA/metal structures are formed using thiol end-groups to orient the ds-DNA in the gaps. The polycation spermidine has been used to stabilize the ds-DNA conformation in the Au/DNA/Au structures. The series of fully complementary DNA double strands illustrated in figure 1 has been studied, in which the G:C segment at the two ends is kept constant while the centre five base pairs are systematically changed from G:C to A:T. The G:C rich end segments are expected to be highly conductive, based on electron transfer and electron transport experiments, and the short alkane thiol linkers are expected to provide strong coupling between the molecule and the metal contacts. The electrical conductivity of the various samples is determined by current–voltage (I – V) measurements performed in a controlled environment.

2. Experimental details

Molecular-scale gaps between Au electrodes (‘nanogaps’, illustrated in figure 2(a)) were fabricated using room-temperature, electromigration-induced breaking of lithographically defined Au lines [27]. Initially, Au microwires of

200 Å thickness were fabricated by e-beam evaporation over a thermally oxidized silicon substrate that was coated with an organic adhesion monolayer [28] of (3-mercaptopropyl) trimethoxysilane (MPTMS) (Sigma-Aldrich, St Louis, MO, USA) (figure 2(b)). A notch was placed at the centre of the microwire to reduce its width to approximately 2 μm in order to localize the break position. A linearly increasing voltage was ramped through these microwires at a step of 20 mV. At a threshold voltage electromigration occurs, during which the Au atoms were pulled out of the high-current-density region. At this point, the Ohmic current through the microwire changes to tunnelling current through the newly formed nanogap, and hence a decrease in current level of several orders of magnitude is observed. Following electromigration, the nanogaps were characterized through field emission scanning electron microscopy (FESEM) imaging using a Hitachi S4800. In addition, the current–voltage characteristics of the gaps were measured using a Keithley 4200 semiconductor characterization system. The nanogap chip was plasma cleaned prior to DNA deposition to remove residual MPTMS or organic contaminants.

The ds-DNA sequences were assembled on the nanogap devices using a four-step chemistry (hybridization, immobilization, stabilization, and cleaning). The DNA sequences were acquired from Integrated DNA Technology (Coralville, IA) and were HPLC purified and MALDI analysed. All the chemicals used in this study were at least ACS grade and the water was prepared with a Millipore UVO purification system (Bedford, MA). The A, A', B, B', C, C', D, and D' 15-base oligonucleotides used in this study are defined in figure 1. Each oligonucleotide was thiolated at its 3' end with a three-carbon-long $-(\text{CH}_2)_3\text{-SH}$ spacer. ds-DNAs thiolated at each 3' end were prepared by mixing together stoichiometric concentrations of two complementary single-stranded DNAs at a concentration of 1 μM in phosphate buffer saline (PBS) solution, i.e. 12 mM $\text{K}_2\text{HPO}_4:\text{KH}_2\text{PO}_4$ at pH 7.2 and either 135 or 500 mM NaCl, and at the stated salt concentrations (either 135 or 500 mM NaCl). Full hybridization was ensured by heating the solution to 90 °C and then allowing it to slowly cool to room temperature. The resulting A:A', B:B', C:C', and D:D' ds-DNAs have a thiol group at each 3' end. The plasma-cleaned electrical break junction chips were immersed in the PBS solution containing the ds-DNAs for 4 h. The strong Au–S bonding between the Au nanoelectrode and the 3'-thiol of DNA helps to immobilize the ds-DNAs in the nanogap. The devices were then exposed to a 1 mM solution of spermidine (obtained from Sigma-Aldrich, St Louis, MO) in PBS for 1 h to stabilize the ds-DNA. The trivalent spermidine polycations (Spd^{3+}) are known to bind to the negatively charged oxygen of phosphate groups in the major or minor grooves of double-stranded DNA and stabilize ds-DNA hybridization [29]. It is believed that the electrostatic interaction between the DNA phosphates and cationic polyamines does not significantly affect either the base pairing or base stacking interactions and does not significantly perturb the native B-form of the DNA [30, 31]. The samples were then thoroughly rinsed with DI to remove any residual salt from the chip and transferred to a 1:4 ethanol:water solution that was gradually replaced with ethanol. The samples were then blown dry with nitrogen to minimize the effect of surface tension upon drying and kept at 4 °C until immediately before the electrical measurements.

3. Results and discussion

FESEM imaging indicates that the nanogaps have molecular scale lengths over approximately 5–15 nm wide regions. Figure 2(c) shows an FESEM image of a nanogap device with sub-5 nm separation. A tunnelling conductance of the order of one nanosiemens (nS) is expected for a nanogap of approximately 1 nm length [27], with decreasing conductance values observed as the gap spacing increases. The 'as-fabricated' nanogap devices used in the current work show a conductance level of one pS or less, which was at the noise level of our instrument, and corresponds to a gap length of approximately 2 nm or more. Based on FESEM imaging, 40% of the total nanogaps exhibited lengths less than 5 nm, with the remainder having lengths between 5 and 15 nm. The nanogap devices are fabricated at room temperature and are relatively stable at the temperatures required for DNA deposition. The MPTMS adhesion layer allows gaps with smaller spacings than those typically achievable with a titanium adhesion layer [27]. The use of the MPTMS molecular adhesion monolayer also eliminates the possibility of residual conduction through the adhesion layer following breaking, which may occur with metal (Ti or Cr) adhesion layers and which would interfere with electrical measurements.

The reaction of single-strand thiolated DNA with Au has been extensively studied [32–34]. It appears that strong Au–DNA interactions are formed by chemisorption of the thiol groups at the 3' ends of the ds-DNA with Au and by the physical adsorption of the amines on the bases with Au. The surface coverage of the dithiol-derivatized ds-DNA was measured using 5'-fluorescein-labelled DNA with the same sequence as A'. The reaction was conducted on a 1 cm² Au surface with all other experimental conditions kept the same as described above. After DNA immobilization, the Au surface was immersed in a 20 mM solution of 1-mercaptoethanol for 24 h, which is known to completely displace the immobilized DNA from the Au surface [35]. The DNA surface coverage was measured from the fluorescence signal in the effluent, which was measured with an excitation wavelength of 480 nm and an emission wavelength of 510 nm using a fluorometer (Perkin Elmer LS-5, Boston, MA). It was found that the final DNA surface coverage was reached within 30 min for both salt concentrations, as shown in figure 3, and equilibrium surface densities of 4×10^{12} and 6×10^{12} DNAs cm⁻² were reached in the 137 mM and 500 mM NaCl–PBS reaction solutions, respectively. We attribute the increase in ds-DNA coverage at high salt concentrations to reduced electrostatic repulsive interactions as the negative charges of DNA phosphate backbone are screened more effectively. The equilibrium coverage results are in reasonable agreement with previously reported values for ds-DNA, which range between 9×10^{12} and 2×10^{13} oligos cm⁻² and appear to be determined by the length and sequence of the DNA [35].

Figure 4 presents the *I*–*V* characteristics of two nanogap devices before and after functionalization with the G:C-rich A:A' ds-DNA at the two NaCl–PBS concentrations. The two lower data sets represent the bare nanogaps; the two upper data sets represent the same devices following functionalization at NaCl concentrations of 137 and 500 mM NaCl, respectively. Conductance increases of $\sim 10^4$ and $\sim 10^6$ were observed upon

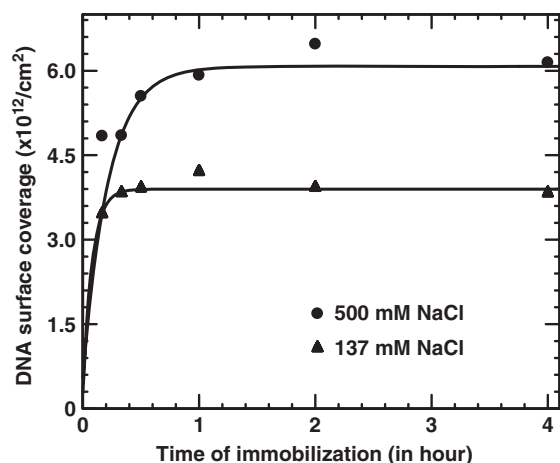


Figure 3. A:A' DNA surface coverage at various NaCl-PBS reaction concentrations as measured with fluorescently labelled A'.

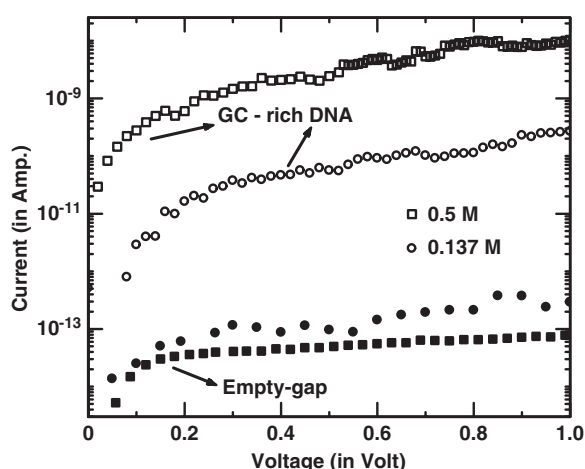


Figure 4. Room-temperature I - V characteristics of bare EIBJ (closed symbols) and EIBJs functionalized with A:A' ds-DNAs (open symbols) in 0.137 mM (circles) and 0.5 mM (squares) NaCl-PBS reaction conditions.

functionalization of the EIBJs with the A:A' ds-DNAs at 137 and 500 mM NaCl concentrations, respectively.

Since various EIBJ devices can have different areas, the number of molecules bridging a specific nanogap (N_{DNA}) is expected to vary from device to device, even at a constant DNA surface coverage. N_{DNA} was estimated from the product of the estimated active area of the nanogap and the surface density of the dithiol-derivatized ds-DNAs. The effective width of each nanogap, i.e. the width over which the separation is 5 nm or less, was determined from FESEM imaging after electrical characterization. The effective area was then taken to be the effective width of the specific device times the thickness of the Au electrodes, and varied from ~ 40 to 100 nm^2 . The estimated number of molecules bridging the gap typically varied from one to six ds-DNAs for deposition at 137 mM NaCl. For the data shown in figure 4, the nanogap device presented for the 0.5 mM NaCl case had an effective area 12 times larger than that of the other device. Coupled with the twofold increase in surface coverage, this difference in area can account for the 30-fold increase in measured conductance. This approach

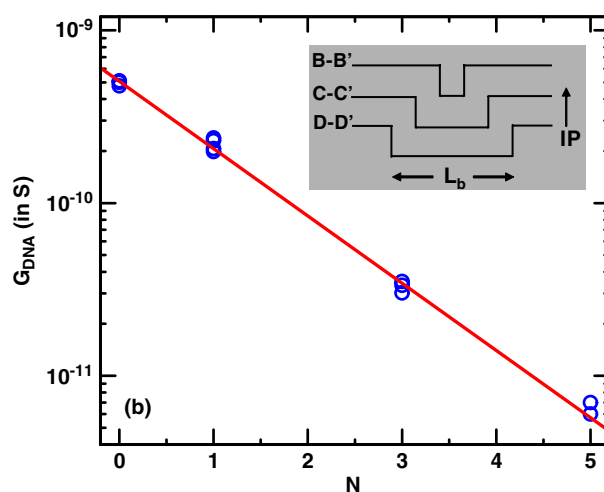
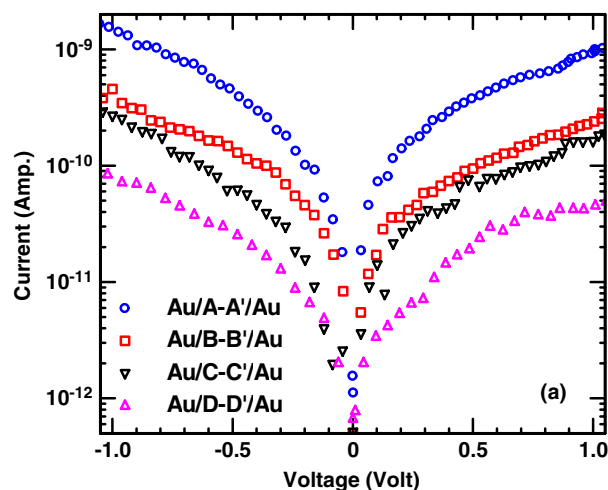


Figure 5. (a) I - V characteristics measured through representative EIBJ devices following immobilization of A:A', B:B', C:C', or D:D' DNA sequences. (b) Measured conductance per molecule (open circles) for EIBJ devices with the various sequences, plotted versus length of the A:T segment. An exponential dependence of G_{DNA} on N has been fitted to these data (solid line), and indicates that the A:T sequence provides a barrier with length equal to L_b . Insets show the relative positions of the highest occupied molecular orbitals of the DNA bases in the various sequences, indicating the barriers to hole flow at the A:T sites.

is based on the assumptions that the surface coverage of ds-DNA in the nanogaps is the same as that on a Au surface and all ds-DNA strands binding within the nanogap actually bridge across the gap, which appears to provide consistent single-molecule electrical transport properties. We note that the tunnelling conductivity of an empty gap does not appear to accurately reflect the 'active area' of the gap, as it is exponentially dependent on the gap spacing. The observation that EIBJ devices with 8–10 nm gaps do not show significant conductivity indicates that the conduction is not due to residual salt in the gap after DNA immobilization and hybridization processing.

Figure 5(a) presents unnormalized I - V characteristics for representative nanogap devices following immobilization of A:A', B:B', C:C', or D:D' at a NaCl concentration of 0.137 M. A $\sim 10^2$ – 10^4 increase in conductivity with respect to

the empty gap current is observed following DNA deposition, with the conductance decreasing as the number of A:T pairs is increased. Figure 5(b) shows the estimated values of the conductance per ds-DNA molecule (G_{DNA}) for multiple devices of configurations A:A' to D:D', calculated by dividing the low-field slopes of the measured I - V curves by the N_{DNA} for the respective device. The use of G_{DNA} allows a direct comparison of the electronic transport properties of the various DNA sequences, as well as comparisons with prior work. The G_{DNA} of $\sim 10^{-9}$ S for the A:A' configurations is consistent with single-molecule conduction measurements, where enhanced conductivity has been observed in G:C-rich DNA [16]. The G_{DNA} is observed to decrease exponentially with increasing length of the A:T segment. A linear fit of the data in figure 5(b) yields the relationship $G_{\text{DNA}} = \alpha G_0 \exp(-\beta L_b)$, where $G_0 = 2e^2/h \approx 77 \mu\text{S}$ is the quantum conductance, $L_b = \delta N$ is the length of the A:T sequence, N is the number of A:T base pairs in the sequence, and δ is the separation distance between base pairs in the DNA double helix (3.4 Å). For this data set, values of $\alpha = 6.38 \times 10^{-6}$ and $\beta = 0.882 \text{ \AA}^{-1}$ are obtained for the extrapolated conductance at zero length (normalized to G_0) and decay constant, respectively. This is comparable with the value of $\beta = 0.97 \text{ \AA}^{-1}$ for A:T hairpins less than 1.7 nm in length inferred from the rate constant in hole transfer experiments [36].

Electronic transport through the π orbitals in ds-DNA is thought to be dominated by hole hopping between G:C base pairs along the length of the DNA molecule [15, 37–39]. Typically, the relative barriers for hopping are attributed to the difference in ionization potential (IP) between the G bases (IP = 8.24 eV) and the other bases, of which the closest is A (IP = 8.44 eV) [40]. The IP of the G:C base pair (IP = 7.76 eV) versus that of the A:T base pair (IP = 8.22 eV) has also been considered [41]; this also indicates that the A:T sequences represent barriers. In addition, the three-hydrogen bonding between G:C base pairs should couple more strongly than the two-hydrogen bonding between A:T base pairs, hence more electronic states for charge transport are expected in G:C base pairs. The observation of $\alpha \ll 1$ indicates that the transport in the A:A' sequence is well away from resonance, as expected from the significant offset between the work function of Au and the IP of the G base. Introducing A:T base pairs at the centre of the DNA strand creates a barrier of length L_b and height ϕ_b equal to the differences in IPs of the substituted bases (approximately 1.1 eV). An approximate energy profile corresponding to the various sequences is shown in the inset of figure 5(b). The exponential dependence of conductivity on L_b is consistent with the expected transmission through a rectangular barrier. While the exponential dependence has been inferred from charge transfer experiments, the result of this experiment provides confirmation that the effect is observed in a transport experiment with constant length DNA. This demonstration could provide a means toward a direct conductance-based approach for DNA sensing.

It is informative to compare and contrast the current results with prior results from electrical transport experiments. Several groups have estimated a conductance of approximately 1 nS for ds-DNA of length 20 nm [42, 43]. A study of conductivity through 8–14-mer, dithiol-functionalized ds-DNA using a scanning tunnelling microscopy (STM) technique

in solution [16] reported a G_{DNA} of 100 nS/oligo for ds-DNA consisting of 5'-CGCGCGCG-3'-thiol and its complement. An inverse relationship was observed between the conductivity and the length of the G:C sequence, which would extrapolate to a value of approximately 20 nS for a 15-base-pair G:C sequence, approximately 30 times larger than the value in the current study. Two factors probably contribute to the enhanced conductivity in the prior experiment. First, theoretical studies have predicted that the presence of counterions, water molecules, structure, and environment will all impact electrical conduction [44]. The spermidine used in our experiment shields the DNA backbone, which may significantly change the local charge environment with respect to that in a buffer solution. The overall results are in qualitative agreement with calculations which predict a reduction in conductivity by removing the water mantle around the ds-DNA strands [45, 46]. Second, the top contact geometry (STM tip) may have resulted in a different tip-to-DNA spacing. The STM study also investigated ds-DNA sequences with A:T pairs inserted in the sequence 5'-CGCG(AT)_mCGCG-3'-thiol, rather than replacing G:C base pairs [16]. In that case, an exponential decrease in conductivity with a decay constant of $\beta = 0.43 \text{ \AA}^{-1}$ was observed for $m \geq 1$. The different value in that study arises, in part, from the fact that the A:T bases are inserted, rather than substituted, within the strand, so that effects due to overall sequence length are included.

The effect of humidity on DNA conductance has been previously studied by various groups [47–50], generally through measurements performed with relatively thick layers of much longer DNAs and using device structures that provide an electrode–electrode separation distance much larger than the length of a single oligonucleotide. In this regime, the overall conductance is dominated by molecule-to-molecule transfer (probably hopping or ion-mediated transport). Exponential increases in conductance values with increases in relative humidity (RH) for poly(GC) and poly(AT) DNAs have been reported, with a $\sim 10^6$ difference in conductance values observed between 5 and 90% RH. The humidity-dependent conductivity and negligible changes between ds- and single-stranded DNA were speculated to be due to ionic conduction in the water layer within the bulk film [47]. Our measurements are performed through well defined device structures with the electrode–electrode separation distances comparable with the length of the 15-bp ds-DNA. After ds-DNA immobilization in a definite nanogap, the devices are exposed to a spermidine environment. This provides a shielding layer over the ds-DNA backbone, which should minimize close interactions with the surrounding atmosphere. In another experiment [51], we have performed the electrical measurements in a nitrogen (N_2) atmosphere and compared to those in ambient conditions. Here, the single ds-DNA conductance values after normalizing by the number of DNAs bridging the nanogap region are comparable for both the situations. This supports the fact that the presence of a spermidine shielding layer over the DNA backbone prevents any interference of absorbed water with the charge flow through the DNA.

4. Conclusions

In conclusion, electrical conduction through dithiol-derivatized ds-DNAs in a nominally dry state has been measured using a

Au/ds-DNA/Au structure suitable for realization of integrated devices. The ds-DNA configuration was immobilized between electrodes within a Au nanogap device and the double-helix configuration was locked with a polycation. The measured conductance data have been normalized to the estimated number of molecules within a specific gap, based on the contact area determined by FESEM imaging and the surface coverage of the ds-DNA molecules. A single ds-DNA conductance of $\sim 10^{-9}$ S is estimated for 15-base-pair G:C-rich ds-DNA. The conductance per ds-DNA molecule was found to decrease exponentially with the length of a sequence of A:T base pairs at the centre of the DNA sequence. While this observation is consistent with prior charge transfer experiments, it had not been previously reported in conductance studies involving constant length DNA sequences. This study shows that changes in the DNA sequence can be detected through changes in the electrical conductance.

Acknowledgments

The authors would like to acknowledge M P Anantram, H Mehrez, and S Datta for informative discussions, and J Choi, Q Hang, and C Y Fong for assistance with FESEM imaging. This work is financially supported by NASA under grant NCC 2-1363 and the NIH Molecular Biophysics pre-doctoral training grant (T32-GM008296).

References

- [1] Steel A B, Herne T M and Tarlov M J 1998 *Anal. Chem.* **70** 4670
- [2] Steel A B, Herne T M and Tarlov M J 1999 *Bioconjugate Chem.* **10** 419
- [3] Drummond T G, Hill M G and Barton J K 2003 *Nat. Biotechnol.* **21** 1192
- [4] Rivas G A, Pedano M L and Ferreyra N F 2005 *Anal. Lett.* **38** 2653
- [5] Seeman N C 2005 *Trends Biochem. Sci.* **30** 119
- [6] LaBean T H, Yan H, Kopatsch J, Liu F, Winfree E, Reif J H and Seeman N C 2000 *J. Am. Chem. Soc.* **122** 1848
- [7] Rinaldi R *et al* 2003 *Appl. Phys. Lett.* **82** 472
- [8] Mao Y, Luo C, Deng W, Jin G, Yu X, Zhang Z, Ouyang Q, Chen R and Yu D 2004 *Nucl. Acids Res.* **32** e144
- [9] Kelley S O and Barton J K 1999 *Science* **283** 375
- [10] Eley D D and Spivey D I 1962 *Trans. Faraday Soc.* **58** 411
- [11] Lewis F D, Liu X, Liu J, Miller S E, Hayes R T and Wasielewski M R 2000 *Nature* **406** 51
- [12] Giese B, Amaudrut J, Kohler A K, Spormann M and Wessely S 2001 *Nature* **412** 318
- [13] Murphy C J, Arkin M R, Jenkins Y, Ghatlia N D, Bossmann S H, Turro N J and Barton J K 1993 *Science* **262** 1025
- [14] Warmana J M, de Haasa M P and Rupprecht A 1996 *Chem. Phys. Lett.* **249** 319
- [15] Dekker C and Ratner M A 2001 *Phys. World* **14** 29
- [16] Xu B Q, Zhang P M, Li X L and Tao N J 2004 *Nano Lett.* **4** 1105
- [17] Storm A J, van Noort J, de Vries S and Dekker C 2001 *Appl. Phys. Lett.* **79** 3881
- [18] de Pablo P J, Moreno-Herrero F, Colchero J, Herrero J G, Herrero P, Baró A M, Ordejón P, Soler J M and Artacho E 2000 *Phys. Rev. Lett.* **85** 4992
- [19] Zhang Y, Austin R H, Kraeft J, Cox E C and Ong N P 2002 *Phys. Rev. Lett.* **89** 198102
- [20] Rakin A, Aich P, Papadopoulos C, Kobzar Y, Vedenev A S, Lee J S and Xu J M 2001 *Phys. Rev. Lett.* **86** 3670
- [21] Cai L, Tabata H and Kawai T 2000 *Appl. Phys. Lett.* **77** 3105
- [22] Yaliraki S N, Kemp M and Ratner M A 1999 *J. Am. Chem. Soc.* **121** 3428
- [23] Emberly E G and Kirczenow G 1998 *Phys. Rev. B* **58** 10911
- [24] Lewis J P, Ordejon P and Sankey O F 1997 *Phys. Rev. B* **55** 6880
- [25] Okahata Y, Kobayashi T, Tanaka K and Shimomura M 1998 *J. Am. Chem. Soc.* **120** 6165
- [26] Iqbal S M, Balasundaram G, Ghosh S, Bergstrom D E and Bashir R 2005 *Appl. Phys. Lett.* **86** 153901
- [27] Mahapatro A K, Ghosh S and Janes D B 2006 *IEEE Trans. Nanotechnol.* **5** 232
- [28] Mahapatro A K, Scott A, Manning A and Janes D B 2005 *Appl. Phys. Lett.* **88** 151917
- [29] Gosule L C and Schellman J A 1976 *Nature* **259** 333
- [30] Gosule L C and Schellman J A 1978 *J. Mol. Biol.* **121** 311
- [31] Deng H, Bloomfield V A, Benevides J M and Thomas G J 2000 *Nucl. Acids Res.* **28** 3379
- [32] Steel A B, Levicky R L, Herne T M and Tarlov M J 2000 *Biophys. J.* **79** 975
- [33] Herne T M and Tarlov M 1997 *J. Am. Chem. Soc.* **119** 8916
- [34] Peterlinz K A, Georgiadis R M, Herne T M and Tarlov M J 1997 *J. Am. Chem. Soc.* **119** 3401
- [35] Demers L M, Mirkin C A, Mucic R C, Reynolds R A III, Letsinger R L, Elghanian R and Viswanadham G 2000 *Anal. Chem.* **72** 5535
- [36] Lewis F D, Zhu H, Daublain P, Fiebig T, Raytchev M, Wang Q and Shafirovich V 2006 *J. Am. Chem. Soc.* **128** 791
- [37] Mehrez H and Anantram M P 2005 *Phys. Rev. B* **71** 115405
- [38] Voityuk A A, Rosch N, Bixon M and Jortner J 2000 *J. Phys. Chem. B* **104** 9740
- [39] Berlin Y A, Burin A L and Ratner M A 2000 *J. Phys. Chem. A* **104** 443
- [40] Hush N S and Cheung A S 1975 *Chem. Phys. Lett.* **34** 11
- [41] Voityuk A A, Jortner J, Bixon M and Rosch N 2000 *Chem. Phys. Lett.* **324** 430
- [42] Shigematsu T, Shimotani K, Manabe C, Watanabe H and Shimizu M 2003 *J. Chem. Phys.* **118** 4245
- [43] Watanabe H, Manabe C, Shigematsu T, Shimotani K and Shimizu M 2001 *Appl. Phys. Lett.* **79** 2462
- [44] Adessi C and Anantram M P 2003 *Appl. Phys. Lett.* **82** 2353
- [45] Endres R G, Cox D L and Singh R R P 2004 *Rev. Mod. Phys.* **76** 195
- [46] Tran P, Alavi B and Gruner G 2000 *Phys. Rev. Lett.* **85** 1564
- [47] Ostmann T K, Jördens C, Baaske K, Weimann T, Angelis M H and Koch M 2006 *Appl. Phys. Lett.* **88** 102102
- [48] Ha D H, Nham H, Yoo K H, So H M, Lee H Y and Kawai T 2002 *Chem. Phys. Lett.* **355** 405
- [49] Gu J, Cai L, Tanaka S, Otsuka Y, Tabata H and Kawai T 2002 *J. Appl. Phys.* **92** 2816
- [50] Armitage N P, Briman M and Grüner G 2004 *Phys. Status Solidi b* **241** 69
- [51] Mahapatro A K, Lee G L, Jeong K J and Janes D B, unpublished